Original Article: Sonocatalytic Degradation of Methyl Red by Sonochemically Synthesized TiO_2-SiO_2/Chitosan Nanocomposite

Robab Mohammadi

Department of Chemistry, Payame Noor University, P.O. BOX 19395-3697, Tehran, Iran

Use your device to scan and read the article online

Citation R. Mohammadi. **Sonocatalytic Degradation of Methyl Red by Sonochemically Synthesized TiO_2-SiO_2/Chitosan Nanocomposite.** *J. Appl. Organomet. Chem.*, **2022**, *2*(4), 188-197.

https://doi.org/10.22034/jaoc.2022.154993

Article info:
Received: 2022-04-22
Accepted: 2022-06-20
Available Online: 2022-07-23

Checked for Plagiarism: Yes
Peer Reviewers Approved by:
Dr.SUNIL V. GAIKWAD
Editor who Approved Publication:
Professor Dr. Abdelkader Zarrouk

Keywords:
TiO_2-SiO_2/chitosan nanocomposite; Sonochemical technique; Sonocatalytic degradation; Methyl red

ABSTRACT

TiO_2-SiO_2/chitosan nanocomposite was synthesized using simple sonochemical technique. The characteristics of the synthesized nanocomposite were examined by TEM, SEM and EDX analysis. The performance of the prepared TiO_2-SiO_2/chitosan nanocomposite as efficient sonocatalyst was investigated for the degradation of methyl red. Sonocatalytic degradation of methyl red in the presence of TiO_2-SiO_2/chitosan nanocomposite could be described via the mechanisms of hot spots and sonoluminescence. The optimized values for main operational parameters were detected as pH of 3, TiO_2-SiO_2/chitosan dosage of 450 mg/L, methyl red initial concentration of 20 mg/L and ultrasonic power of 300 W. Under optimal conditions, the sonocatalytic degradation of methyl red was 99.1 %. Based on the obtained results, TiO_2-SiO_2/chitosan nanocomposite could be an excellent selectivity for sonocatalytic degradation of anionic dyes such as methyl red.

Introduction

Waste-water from textile industry always contains pigments or dyes, which may cause severe environmental pollution; so, the water decontamination became one of the most urgent problems that need to be studied and dissolved [1]. Therefore, different methods such as adsorption, ion exchange, nanophotocatalysis, membrane and ultrasonic technologies, electrocoagulation, coagulation and enhanced coagulation have been used for the degradation of pollutants from water, among which the advanced oxidation processes (AOPs) have been known as an efficient method for the degradation of the organic pollutants compared to other methods. Preparation of hydroxyl radicals with high oxidative potential in AOPs has caused these

*Corresponding Author: Robab Mohammadi (mohammadi_rb@yahoo.com)

treatment procedures to be introduced as one of the most practical physicochemical treatment processes [2-4]. Because of the non-selective function and high oxidative power at normal temperature and pressure, hydroxyl radical is capable of oxidizing almost all the reduced materials unlimitedly. Among all the AOPs, today, the focus is on usage of ultrasonic irradiation as a result of its high efficiency in the removal of resistant industrial pollutants, high power for degradation of the persistent organic pollutants, as well as easiness and safety of exploitation. The influence of sonication is the direct result of the formation of cavitation microbubbles [5]. The produced microbubbles.

grow with ultrasonic frequency and when the resonance frequency size reaches a critical value, the collapse of bubbles occurs [6]. These conditions may dissociate water molecules to produce hydrogen and hydroxyl radicals. Hydroxyl radicals are powerful oxidizing agents which can attack and destroy almost all organic pollutants to smaller molecules and finally convert them mainly to H_2O and CO_2 [7]. Removal of organic pollutants *via* ultrasonic irradiation is time-consuming and needs fairly large amount of energy. In order to overcome this shortcoming of ultrasonic degradation, a broad attention has been paid to the application of semiconductors as catalysts in the sonocatalytic procedure, which can enhance the performance of the removal procedure [8]. The influence of catalyst may be related to the synergistic influences of sonolysis combined with the heterogeneous semiconductor [9]. The semiconductor particles enhance the mass transfer coefficient of organic pollutants between the liquid and the surface of the sonocatalyst. Also, the presence of the sonocatalyst may provide additional active sites for nucleation of bubbles [10]. As well known, various materials have been applied as suitable sonocatalysts; for instance, TiO_2, ZnO, CdSe, ZnS, and SiO_2. Recently, TiO_2 has been widely used in the sonocatalytic procedure for removal of organic contaminants owing to its exceptional chemical and physical properties, non-toxicity and low cost [11]. To date, various studies have been conducted among which the usage of mixed oxide such as TiO_2/SiO_2 is more useful than that of TiO_2. The available surface area of TiO_2 may be increased *via* the addition of SiO_2. So, adsorption of contaminant molecules on the surface of silica can be enhanced; therefore, the catalytic activity of TiO_2 may be improved [12]. Moreover, the addition of SiO_2 enhances the content of surface adsorbed water and hydroxyl groups that affect the catalytic activity of TiO_2/SiO_2 mixed oxides [13].

The application of polymeric matrixes such as alginate, chitosan and various resins is one of the most widely used processes for the immobilization. Chitosan is a suitable natural biopolymer for the immobilization process because of its hydrophilicity, biodegradability, non-toxicity and availability. Moreover, adsorption capacity of the chitosan for sequestering anionic dyes because of the electrostatic attraction between the protonated amine groups on the chitosan and the sulfonic groups of the anionic dyes is beneficial to enhance the adsorption of anionic dyes together with the immobilized adsorbent [14].

Several preparation methods have been suggested by various researchers including sol-gel, sonochemical, hydrothermal and electrochemical techniques. However not much work has been reported on the preparation of TiO_2-SiO_2/chitosan nanocomposite *via* sonochemical method.

The aim of the present paper was to prepare TiO_2-SiO_2/chitosan nanocomposite *via* simple sonochemical method as an efficient sonocatalyst for the treatment of methyl red solution. SEM, EDX, and TEM analysis were carried out to characterize TiO_2-SiO_2/chitosan nanocomposite. Subsequently, the sonocatalytic activity of TiO_2-SiO_2/chitosan nanocomposite was investigated for the methyl red degradation. Also, the influence of important factors such as the solution pH, TiO_2-SiO_2/chitosan nanocomposite dosage, initial pollutant concentration and ultrasonic power was studied on the degradation efficiency of methyl red.

Experimental

Plant material

Titanium n-butoxide (TBOT), tetraethyl orthosilicate (TEOS), oxalic acid, methyl red, and ethanol were purchased from Merck Co (Germany). Chitosan, which was of analytical grade, was purchased from Sigmae Aldrich, USA.

Synthesis of TiO_2/SiO_2 nanocomposite by sonochemical method

For TiO_2 sol production, TBOT (5 mL) was added dropwise into ethanol (20 mL), previously stirred under an inert nitrogen atmosphere for 5 min. For SiO_2 preparation, sonotrode equipment (Hielscher Ultrasound Technology UP200Ht, Teltow, Germany) was used. A solution of distillated water (6 mL), absolute ethanol (20 mL) and oxalic acid (0.33 mL), in a 5:5:0.1 molar relations was prepared and stirred sonochemically for 15 min. Afterwards, TEOS (15 mL) was added dropwise and the mixture was stirred sonochemically for 3 min. The molar ratio of TEOS/EtOH was 1:5. Finally, TiO_2 sol and SiO_2 sol were mixed. Immediately after mixing, 10 mL of distilled water was added and mixed continuously using sonotrode conditions for 20 min. The resultant mixture was left to be dried at room temperature.

Preparation of TiO_2/SiO_2 -chitosan nanocomposite

To prepare TiO_2/SiO_2 -chitosan nanocomposite, first chitosan (8 g) was dissolved in 1000 mL of 1 M acetic acid and then mixed using magnetic stirrer at 100 rpm for 2 h. Then, TiO_2/SiO_2 (4 g) was added to the concentrated solution and mixed continuously using sonotrode conditions for 50 min to reach homogeneity. The resulted mixture was kept for 8 h in a stable place. The weight ratio of chitosan to TiO_2/SiO_2 was 2:1. The mixture was added dropwise via a syringe to a mixture solution of NaOH (1.3 mL) and ethanol (20 mL). The molar ratio of NaOH/ethanol was 1:5. Then, they were stored in the solution for 24 h to allow the nanocomposite to be formed. The resulted sample was withdrawn from the solution and washed with deionized water several times to remove impurities. The obtained nanocomposite was dried in room temperature.

Results and Discussion

Characterization of TiO_2/SiO_2 and TiO_2/SiO_2 -chitosan catalysts

SEM was applied to investigate the surface morphology of the prepared samples. SEM micrographs of TiO_2/SiO_2 and TiO_2/SiO_2-chitosan are shown in Figure 1. Figure 1a shows smooth and bulky morphology of TiO_2/SiO_2. However, Figure 2b for TiO_2/SiO_2-chitosan implies the presence of fine spherical nanostructures. With simple comparison of the SEM images of TiO_2/SiO_2 with that of TiO_2/SiO_2 -chitosan, it is obviously observed that TiO_2/SiO_2 nanoparticles were synthesized and immobilized on the chitosan surface. Raut et al. studied the compatibility between chitosan and TiO_2 using Fourier transform infrared spectrometry. They reported that TiO_2 particles had good compatibility with chitosan, because there were many hydroxyl groups on the surface of TiO_2, which formed hydrogen bonds with the hydroxyl groups in the chitosan [15]. In this work, It is apparent that physical interaction, mainly H-bonding, is responsible for binding the components into the chitosan matrix. It is concluded that hydroxyl groups on the surface of TiO_2/SiO_2 can form hydrogen bonds with the hydroxyl groups in the chitosan.

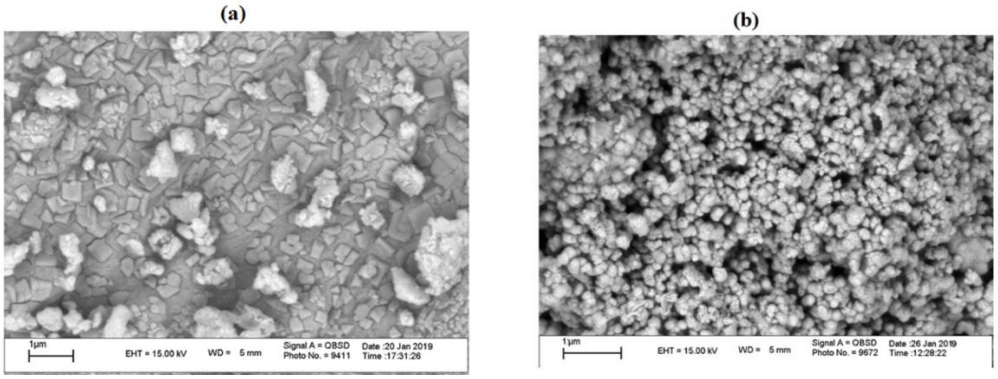

Figure 1. SEM images of (a) TiO_2/SiO_2 and (b) TiO_2/SiO_2-chitosan samples

EDX diffraction of TiO_2/SiO_2-chitosan nanocomposite was depicted in Figure 2. As shown in Figure 2, the presence of the obvious peaks related to C, O, N, Ti and Si compounds are evident. EDX analysis demonstrated no significant levels of impurities which could have been produced from the procedure [16].

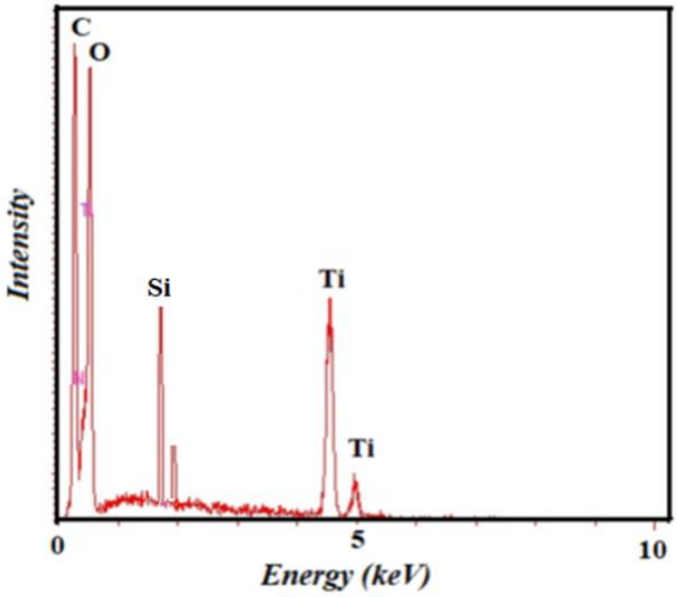

Figure 2. EDX spectrum of TiO_2/SiO_2-chitosan nanocomposite

The morphology of TiO_2/SiO_2-chitosan nanocomposite was also investigated by TEM. Figure 3 shows a relatively uniform particle size distribution with crystallite size below 25 nm. From TEM image, chitosan layers on the TiO_2/SiO_2 surface attached together and produced the porous structure. The porous structure of chitosan on the TiO_2/SiO_2 surface may be an important factor that permits specific interactions of TiO_2/SiO_2-chitosan nanocomposite with pollutant molecules, making it an important feature for the sonocatalytic performance [17].

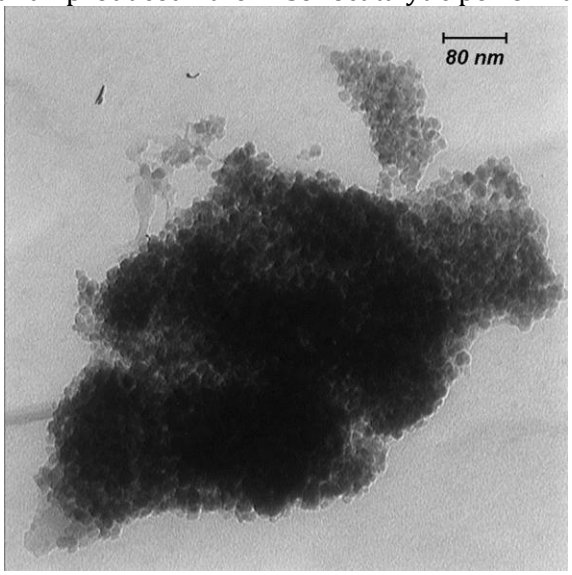

Figure 3. TEM image of TiO_2/SiO_2-chitosan nanocomposite

Degradation of methyl red in different processes

Figure 4 displays the comparison of various procedures performance for degradation of methyl red. The DR% was found to be low (11 %) as methyl red was exposed to sonication at ultrasonic power of 300 W for 20 min. This may be due to the low rate of hydroxyl radical generation *via* sonolysis alone. Also, the adsorption of methyl red on the TiO_2/SiO_2-chitosan did not show a considerable removal of methyl red after 20 min. However, the DR% was 38%, 69.8% and 99.1% for sonocatalysis with TiO_2, TiO_2/SiO_2 and TiO_2/SiO_2-chitosan samples, respectively. This improvement can be attributed to the increment in numbers of cavitation bubble which occurs on the surface of the nanocomposite and resulted in water cleavage and production of more hydroxyl radicals. The high DR% of methyl red by sonocatalytic procedure in the presence of TiO_2/SiO_2-chitosan can be also due to the sonoluminescence mechanism. Sonoluminescence involves an intense UV-light, which excites TiO_2/SiO_2-chitosan nanocomposite to behave as an efficient photocatalyst during ultrasonic illumination [18].

The beneficial influence of SiO_2 may be ascribed to its ability to adsorb more hydroxyl radicals. The acidity of the binary oxide may be enhanced *via* adding SiO_2 in TiO_2. The increase in acidity has been described by the model proposed by Guan [19]. According to this model, doped SiO_2 cation enters the lattice of TiO_2, and retains its original coordination number. The doped cation is still bonded to the same number of oxygen atoms despite coordination variations in the oxygen atoms, and so, a charge imbalance may be generated. However, the charge imbalance must be satisfied. So, Lewis sites can be produced because of the positive charge in TiO_2/SiO_2. The surface with improved acidity can adsorb more hydroxyl radicals which led to increase the catalytic activity and complete degradation of methyl red.

From Figure 4, sonocatalytic activity of TiO_2/SiO_2-chitosan is considerably higher than that of TiO_2/SiO_2. The incorporation of TiO_2/SiO_2 with Ti-OH and Si-OH groups into chitosan with positively charged amino groups led to the grafting of these functional groups which is desirable for the adsorption of methyl red containing negatively charged carboxilic groups.

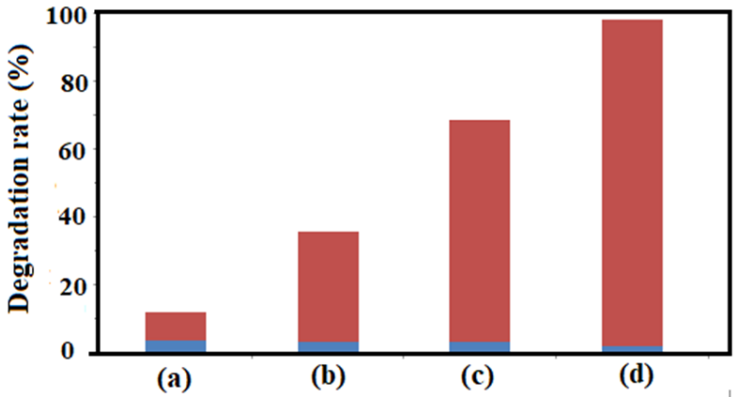

Figure 4. Sonocatalytic degradation of methyl red in the presence of (a) US only, (b) TiO_2, (c) TiO_2/SiO_2, and (d) TiO_2/SiO_2-chitosan. Experimental conditions: pH = 3, $[dye]_0$ =20 mg/L, [Catalyst] = 450 mg/L and ultrasonic power = 300 W.

Effects of the operational parameters on the degradation of methyl red in US-TiO_2/SiO_2-chitosan process

The effect of the main factors including pH of the solution, TiO_2/SiO_2-chitosan dosage, initial concentration of pollutant, and ultrasonic power on the methyl red degradation was investigated. It is well known that pH is one of the main variables influencing the degradation of organic dyes in sonocatalytic procedures. Therefore, experiments were performed to study the effect of pH on the

DR% of methyl red. The influence of varying the initial pH value of methyl red solution on sonocatalytic degradation was demonstrated in Figure 5 (A). In order to study the influence of pH value of methyl red solution, four different pH values (initially at 3, 5, 7 and 9) of methyl red were selected. Based on the results, the sonocatalytic degradation efficiency was faster in an acidic media than in alkaline media and the most effective degradation rate was pH = 3.

Methyl red has a high concentration in the bubble interface in an acidic pH, therefore it was more vulnerable to the hydroxyl radical attack. Acidic media accelerate degradation, this acceleration can be attributed to the hydrophobic character of the protonated negatively charged -COO^- group in acidic media, which increases its reactivity under ultrasound treatment. Moreover, the composition of methyl red would change to the quinone type, which is unstable and easy to be destroyed under pH= 3, when the pH value is greater than 4.4, the azo bond is strong and difficult to be destroyed [20]. The surface of TiO_2/SiO_2-chitosan was negatively charged at pH values above pH_{pzc} (7.5) and positively charged at pH values below 7.5; then, at acidic pHs, adsorption of the anionic dye on the positively charged surface of TiO_2/SiO_2-chitosan was facilitated, which resulted in degradation of more methyl red molecules *via* the produced hydroxyl radicals. Also, the oxidation potential of hydroxyl radicals decreases from E= 2.8 V to E= 1.95 V when pH increases from 0 to 14 [21].

Figure 5 (B) demonstrates a series of experimentations performed *via* changing the amount of TiO_2/SiO_2-chitosan from 150 to 450 mg/L. An increment in the sonocatalyst loading up to 450 mg/L resulted in an improvement in DR%. This improvement can be related to the increase in available active surface area, which in turn increased the generation of cavitation bubbles and promoted the sonoluminescence phenomenon [22].

Tabriz, Iran. The results in Figure 5 (E) display the influence of presence of common anions such as sulfate, carbonate, and bicarbonate on the ultrasonic degradation of methyl red. As can be seen in presence of sulfate, carbonate, and

The effect of initial concentration (20, 30, 40 and 50 mg/L) of methyl red on the degradation efficiency was investigated. Figure 5 (C) shows the DR% decreases as the initial reactant concentration increases. The possible reason for this phenomenon could be related to the fact that when the initial concentration is enhanced, more pollutant molecules can be adsorbed on the surface of the catalyst, thus all the surface sites for the adsorption of hydroxyl ions are blocked and there is very low availability of the sites for the new formation of hydroxyl radicals. Consequently, the sonocatalytic degradation efficiency of methyl red is declined. Furthermore, as the dye concentration was enhanced and other operational parameters were fixed, the same numbers of reactive oxygen species were formed, which had to degrade more pollutant molecules and the intermediates produced *via* their decomposition; as a consequence, the DR% significantly decreased as the pollutant concentration increased.

Figure 5 (D) displays the sonocatalytic degradation of methyl red at ultrasonic powers of 200 and 300 W using TiO_2/SiO_2-chitosan nanocomposite. The solution turbulence and coefficient of mass transfer was increased *via* increasing ultrasonic power from 200 to 300 W [23]. The probable cause of this phenomenon is that the formation, growth, and rupture of cavitation bubbles in liquids were easier to complete under the condition of stirring ultrasound [24]. A large number of light and heat formed *via* the rupture of cavitation bubbles was transmitted to the surface of the catalyst, which greatly enhances the degradation rate [25].

In order to study the efficiency of TiO_2/SiO_2-chitosan nanocomposite in ultrasonic degradation of methyl red in the real water, 20 mg/L of dye was added into a real water sample (carbonate hardness: 87 mg/L $CaCO_3$, sulfate concentration: 173 mg/L SO_4^{2-}) that was obtained from an irrigation well in

bicarbonate, the percentage of degradation decreases. This inhibition is undoubtedly because of their ability to act as hydroxyl radical's scavengers by the following reactions [26-28]:

$$SO_4^{2-} + OH^{\cdot} \rightarrow SO_4^{-\cdot} + OH^- \qquad (1)$$

$$HCO_3^- + OH^{\cdot} \rightarrow CO_3^{-\cdot} + OH^- \qquad (2)$$

$$CO_3^{2-} + OH\cdot \rightarrow CO_3^{-\cdot} + OH^- \qquad (3)$$

These ions may also block the active sites on the TiO_2/SiO_2-chitosan surface thus deactivating the catalysts towards dye and intermediate molecules. Although the formed radical anions have been shown to be an oxidant itself, its oxidation potential is less than that of the hydroxyl radicals.

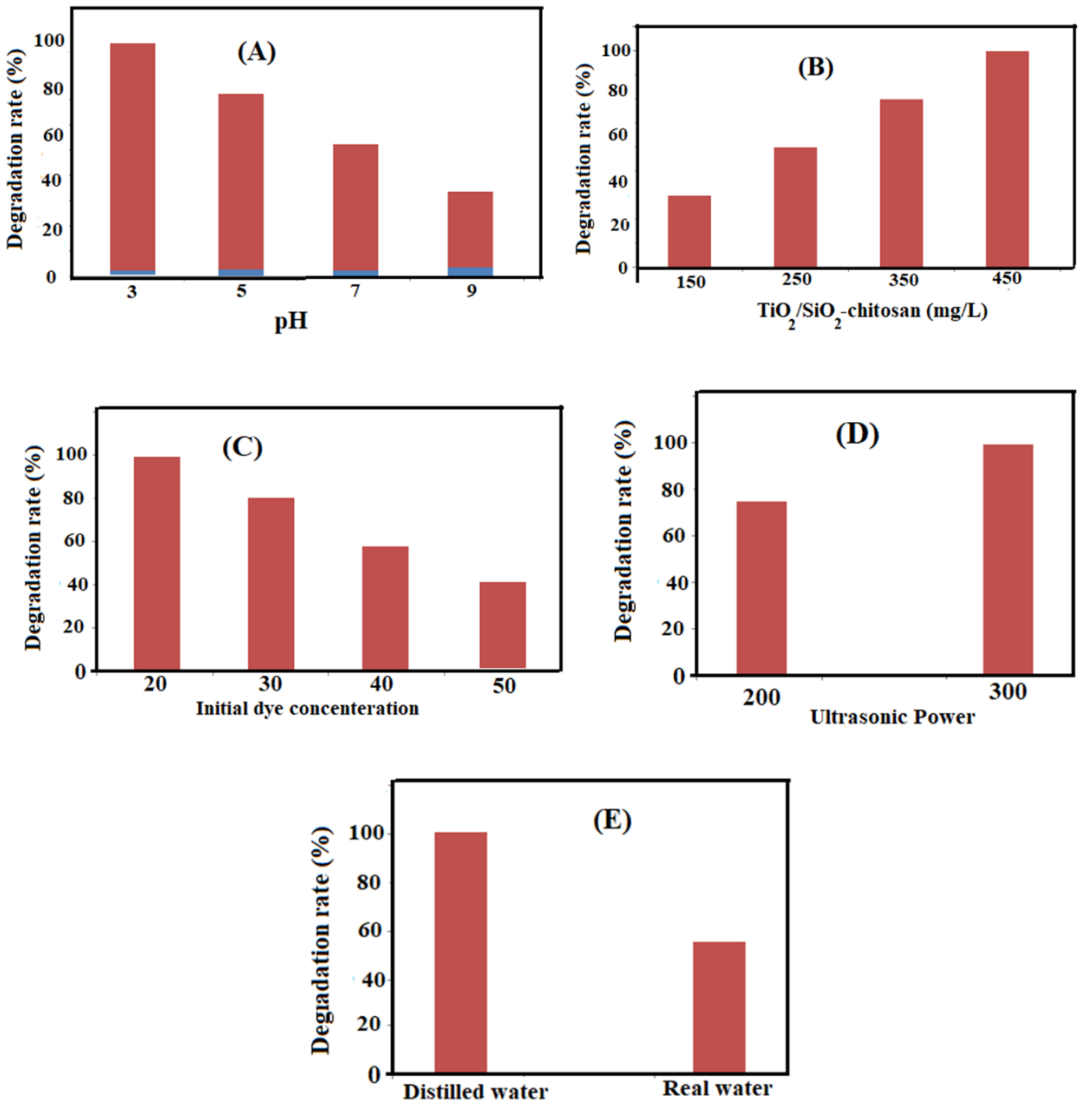

Figure 5. Influence of operation parameters on degradation rate of methyl red in the US-TiO_2/SiO_2-chitosan process; (A) Influence of pH ($[dye]_0$ = 20 mg/L, [Catalyst] = 450 mg/L and ultrasonic Power = 300 W); (B) Influence of TiO_2/SiO_2-chitosan dosage (pH =3, $[dye]_0$ = 20 mg/L and ultrasonic power = 300 W); (C) Influence of dye concentration (pH =3, [Catalyst] = 450 mg/L and ultrasonic power = 300 W); (D) Influence of ultrasonic power (pH = 3, $[dye]_0$ = 20 mg/L and [Catalyst] = 450 mg/L); (E) Investigation of the efficiency of TiO_2/SiO_2-chitosan in degradation of methyl red from real water (pH = 3, $[dye]_0$ = 20 mg/L, [Catalyst] = 450 mg/L and ultrasonic power = 300 W).

Proposed degradation mechanisms

The ultrasonic degradation mechanism of methyl red on TiO_2/SiO_2-chitosan nanocomposite can be explained as follows:

First, water, O_2, and methyl red are adsorbed on the surface of TiO_2/SiO_2-chitosan nanocomposite, followed by the generation of hole-electron pairs on nanocomposite surface as the light energy to overcome the band gap energy between valence band and conduction band [29]. So, the electrons excited from the nanocomposite surface will transfer from the valence band into the conduction band [30]. Then, the hydroxyl radicals with strong oxidizing activity further react with and degrade methyl red into small molecules. The high DR% of methyl red by sonocatalytic process in the presence of TiO_2/SiO_2-chitosan may be also due to the sonoluminescence mechanism. Sonoluminescence involves an intense UV-light, which excites TiO_2/SiO_2-chitosan nanocomposite to behave as an efficient sonocatalyst during ultrasonic irradiation [31]. The reaction mechanism between methyl red and TiO_2/SiO_2-chitosan is summarized from Equation (4) to Equation (8). The methyl red degradation mechanism included: (1) Adsorption, the electrostatic attraction between–NH_3^+ group of chitosan and $-COO^-$ of methyl red molecules; (2) sonocatalysis, the sonocatalytic degradation of methyl red by ultrasonic illumination began with excitation of TiO_2 and then formed an electron-hole pair (Equation (4)). High oxidation valence-band holes (h^+) directly oxidized methyl red degradation (Equation (5)). Water decomposition produced OH radicals (Equation (6)) or a reaction of h^+ with OH^- (Equation (7)). Meanwhile, the reaction between conduction-band electrons (e^-) and proper electron acceptors (such as O_2) yielded oxidative radicals as described by Equation (8). The generated hydroxyl radicals easily degraded methyl red to form inorganic small molecules (Equation (9)) [32,33].

$$TiO_2 + h\vartheta \rightarrow h_{vb}^+ + e_{cb}^- \quad (4)$$

$$h_{vb}^+ + methyl\ red \rightarrow Oxidation\ of\ methyl\ red \quad (5)$$

$$h_{vb}^+ + H_2O \rightarrow H^+ + OH^{\cdot} \quad (6)$$

$$\boldsymbol{OH^- + h_{vb}^+ \rightarrow OH^{\cdot}} \quad \textbf{(7)}$$

$$e_{cb}^- + O_2 \rightarrow O_2^{\cdot -} \quad (8)$$

$$OH^{\cdot}/O_2^{\cdot -} + methyl\ red \rightarrow Degradation\ of\ methyl\ red$$

When a colored organic compound is adsorbed on the surface of TiO_2/SiO_2-chitosan nanocomposite, a sensitized catalytic procedure is possible. Huang *et al.* studied dye sensitized degradation which follows the radical mechanism [34]. In dye-sensitization, an organic dye absorbing light excites an electron from the HOMO (highest occupied molecular orbital) of a dye to the LUMO (lowest unoccupied molecular orbital) [35]. LUMO level of methyl red is more negative relative to the conduction band edge potential of TiO_2. Therefore, because of the more negative potential of the adsorbed oxygen through capturing electrons from the conduction band of the catalyst. The $\cdot O_2^-$ can react with surface adsorbed H_2O to produce H_2O_2 which is ultimately converted to ·OH [37]. The surface adsorbed dye radical cation or surface lowest unoccupied molecular orbital (LUMO) level for methyl red relative to the conduction band (CB) of the catalyst, the electron transfer from the LUMO of dye to the CB of the catalyst is feasible. It is reported that the redox potential of $O_2/\cdot O_2^-$ is −0.33 V vs. NHE, which is more positive than conduction band potential of TiO_2 (−0.5 V vs NHE [36]. The surface adsorbed methyl red was excited *via* absorbing light and donated electrons to the conduction band of the catalyst. As a result, methyl red is converted to a cationic radical (dye+·), and $\cdot O_2^-$ radical specie were easily generated *via* the adsorbed dye can undergo degradation *via* $\bullet O_2^-$ and ·OH. As soon as a dye molecule degrades, another dye molecule will be adsorbed on catalyst surface and the catalytic cycle continues. It is reported that azo bonds are more reactive than

the aromatic part of the molecule. They can be easily oxidized *via* the photogenerated OH radicals. The cleavage of the azo (–N=N–) bond leads to decolorization of methyl red [38]. The possible degradation pathway of methyl red was proposed in Figure 6.

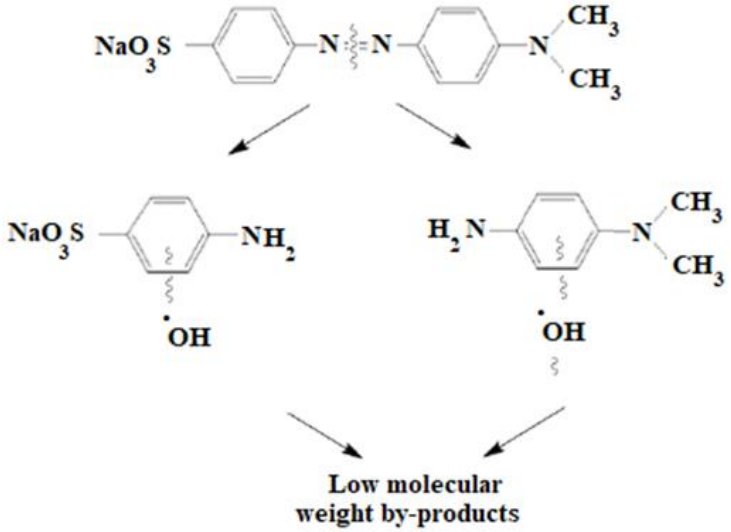

Figure 6. Proposed degradation pathway of methyl red by the synthesized nanocomposite

Conclusion

TiO_2/SiO_2-chitosan nanocomposite was prepared by Sonochemical technique and characterized *via* TEM, SEM and EDX analysis. TiO_2/SiO_2-chitosan presented high sonocatalytic performance for degradation of methyl red. Degradation efficiency of 99.1 % was observed at solution pH of 3, TiO_2/SiO_2-chitosan loading of 450 mg/L, initial dye concentration of 20 mg/L and ultrasonic power of 300 W. The degradation efficiency significantly declined in the presence of various anions such as sulfate, carbonate, and bicarbonate, confirming the role of % OH radicals in the US/TiO_2/SiO_2-chitosan procedure. These results show the potential of TiO_2/SiO_2-chitosan nanocomposite for sonocatalytic degradation of organic pollutants.

Acknowledgements

The author thanks Payame Noor University I.R. of Iran for all the support.

References

[1] G.S. Lakshmi, Performance analysis of multi-level diode-clamped inverter fed IPMSM drive for electric vehicles. In *2018 IEEE Innovative Smart Grid Technologies-Asia (ISGT Asia).* IEEE. 2018, 54-61. [Crossref], [Google Scholar], [Publisher]
[2] Z. Khani, D. Schieppati, C.L. Bianchi, D.C. Boto, *Catalysts,* **2019**, *9*, 1-20. [Crossref], [Google Scholar], [Publisher]
[3] A. Rosales, A. Maury-Ramírez, R.M.D. Gutiérrez, C. Guzmán, K. Esquivel, *Coatings,* **2018**, *8*, 1-13. [Crossref], [Google Scholar], [Publisher]
[4] R. Mohammadia, M. Isazadeh, *Asian J. Green Chem.,* **2019**, *3*, 432-454. [Crossref], [Google Scholar], [Publisher]
[5] N. Yuan, G. Zhang, S. Guo, Z. Wan, *Ultrason. Sonochem.,* **2016**, *28*, 62–68. [Crossref], [Google Scholar], [Publisher]
[6] X. Hu, Q. Zhu, Z. Gu, N. Zhang, N. Liu, M.S. Stanislaus, D. Li, Y. Yang, *Ultrason. Sonochem.*, **2017**, *36*, 301–308. [Crossref], [Google Scholar], [Publisher]
[7] R.D.C. Soltani, S. Jorfi, H. Ramezani, S. Purfadakari, *Ultrason. Sonochem.,* **2016**, *28*, 69–78. [Crossref], [Google Scholar], [Publisher]

[8] R. Mohammadia, N. Sabourmoghaddam, *Asian J. Green Chem.*, **2020**, *4*, 11-32. [Crossref], [Google Scholar], [Publisher]
[9] W. Sangchay, *Energy Procedia.,* **2016**, *89*, 170–176. [Crossref], [Google Scholar], [Publisher]
[10] A. Khataee, R. Honarnezhad, M. Fathinia, *J. Environ. Manage.,* **2018**, *211*, 225-237. [Crossref], [Google Scholar], [Publisher]
[11] S. Song, C. Hao, X. Zhang, Q. Zhang, R. Sun, *Open Chem.,* **2018**, *16*, 1283-1296. [Crossref], [Google Scholar], [Publisher]
[12] R. Huang, Q. Liu, J. Huo, B. Yang, *Arab. J. Chem.,* **2017**, *10*, 24-32. [Crossref], [Google Scholar], [Publisher]
[13] Z. He, C. Sun, S. Yang, Y. Ding, H. He, Z. Wang, *J. Hazard Mater.,* **2009**, *162*, 1477–1486. [Crossref], [Google Scholar], [Publisher]
[14] R. Mohammadi, N. Sabourmoghaddam, *Asian J. Green Chem.,* **2020**, *4*, 107-120. [Crossref], [Google Scholar], [Publisher]
[15] AV. Raut, H.M. Yadav, A. Gnanamani, S. Pushpavanamd, S.H. Pawar, *Colloids and Surfaces B: Biointerfaces*, **2016**, *148*, 566-575. [Crossref], [Google Scholar], [Publisher]
[16] T. Thi, T. Nguyen, O. Hee, J. Seo, *Carbohydr. Polym.,* **2011**, *86*, 1799-1806. [Crossref], [Google Scholar], [Publisher]
[17] I.W. Nam, H.K. Kim, H.K. Lee, *Constr. Build. Mater.,* **2012**, *30*, 480-487. [Crossref], [Google Scholar], [Publisher]
[18] A. Khataee, H. Marandizadeh, B. Vahid, M. Zarei, S.W. Joo, *Chem. Eng. Process.*, **2013**, *73*, 103–110. [Crossref], [Google Scholar], [Publisher]
[19] K. Guan, *Surf. Coat. Technol.,* **2005**, *191*, 155–160. [Crossref], [Google Scholar], [Publisher]
[20] R. Mohammadi, B. Massoumi, *Russ. J. Phys. Chem. A.*, **2014**, *88*, 1184–1190. [Crossref], [Google Scholar], [Publisher]
[21] M. Zeng, *Bull. Korean Chem. Soc.* **2013**, *34*, 953-956. [Crossref], [Google Scholar], [Publisher]
[22] I.V. Lightcap, T.H. Kosel, P.V. Kamat, *Nano Lett.,* **2010**, *10*, 577–583. [Crossref], [Google Scholar], [Publisher]
[23] M. Stucchi, G. Cerrato, C.L. Bianchi, *Ultrason. Sonochem.,* **2019**, *51*, 462–468. [Crossref], [Google Scholar], [Publisher]
[24] J. Wang, B. Guo, X. Zhang, Z. Zhang, J. Han, J. Wu, *Ultrason. Sonochem.,* **2005**, *12*, 331-337. [Crossref], [Google Scholar], [Publisher]
[25] N. Bayal, P. Jeevanandam, *Ceram. Int.,* **2014**, *40*, 15463-15477. [Crossref], [Google Scholar], [Publisher]
[26] A.M.M. Ahmeda, A.E. Alib, A.H. Ghazy, *Adv. J. Chem. A.*, **2019**, *2*, 79-93. [Crossref], [Google Scholar], [Publisher]
[27] S. Sheshmani, A. Ashori, S. Hasanzadeh, *Int. J. Biol. Macromol.,* **2014**, *68*, 218-224. [Crossref], [Google Scholar], [Publisher]
[28] S. Tabasideh, A. Maleki, B. Shahmoradi, E. Ghahremani, G. Mckay, *Sep. Purif. Technol.,* **2017**, *189*, 186-192. [Crossref], [Google Scholar], [Publisher]
[29] M. Hamadanian, A. Reisi-Vanani, A. Majedi, *J. Iranian. Chem. Soc.,* **2017**, *1*, S52–S58. [Crossref], [Google Scholar], [Publisher]
[30] A.J. Haider, R.H. AL–Anbari, G.R. Kadhim, C.T. Salame, *Energy Procedia.,* **2017**, *119*, 332–345. [Crossref], [Google Scholar], [Publisher]
[31] L. Liu, Y. Li, *Aerosol. Air Qual. Res.,* **2014**, *14*, 453-469. [Crossref], [Google Scholar], [Publisher]
[32] K. Ishibashi, A. Fujishima, T. Watanabe, K. Hashimoto, *Electrochem. Commun.,* **2000**, *2*, 207–210. [Crossref], [Google Scholar], [Publisher]
[33] J. Ananpattarachai, P. Kajitvichyanukul, S. Seraphin, *J. Hazard. Mater.,* **2009**, *168*, 253- 261. [Crossref], [Google Scholar], [Publisher]
[34] S.T. Huang, Y.R. Jiang, S.Y. Chou, Y.M. Dai, C.C. Chen, *J. Mol. Catal. A Chem.,* **2014**, *391*, 105–120. [Crossref], [Google Scholar], [Publisher]
[35] M.A.I. Molla, I. Tateishi, M. Furukawa, H. Katsumata, T. Suzuki, S. Kaneco, *Open J. Inorg. Non Met. Mater.,* **2017**, *7*, 1–7. [Crossref], [Google Scholar], [Publisher]
[36] H. Park, Y. Park, W. Kim, W. Choi, J. *Photochem. Photobiol. C Photochem. Rev.,* **2013**, *15*, 1–20. [Crossref], [Google Scholar], [Publisher]
[37] L.G. Devi, S.G. Kumar, *Appl. Surf. Sci.*, **2012**, *261*, 137–146. [Crossref], [Google Scholar], [Publisher]
[38] K. Zaja, J. Choina, D. Dolat, A. Morawski, *Pol. J. Environ. Stud.*, **2010**, *19*, 685– 691. [Google Scholar], [Publisher]